Near-Optimum Iterative Multiuser Detection in Time-Frequency-Domain Spread Multicarrier DS-CDMA Systems

Peng Pan and Lie-Liang Yang
School of ECS, University of Southampton
SO17 1BJ, United Kingdom
Tel: 0044-(0)23-8059 3364, Email: pp07v,lly@ecs.soton.ac.uk
http://www-mobile.ecs.soton.ac.uk

Youguang Zhang
School of Electronic and Information Engineering
Beihang University
Beijing 100083, China
Email: zhangyouguang@vip.sina.com

***Abstract*— In this contribution we propose and study a novel iterative time-frequency-domain (TF-domain) multiuser detector (MUD) for the multicarrier direct-sequence code-division multiple-access system employing both T-domain and F-domain spreading, which, for brevity, is referred to as the TF/MC DS-CDMA system. The proposed iterative TF-domain MUD consists of a set of T-domain soft-input soft-output MUDs (SISO-MUDs) and a set of F-domain SISO-MUDs, which exchange information through two multiuser interference (MUI) cancellation units. Both the T-domain and F-domain SISO-MUDs are operated under the maximum *a-posteriori* (MAP) principles. In this contribution the complexity and bit error rate (BER) performance of the TF/MC DS-CDMA employing the proposed iterative TF-domain MUD are investigated and also compared with the other existing MUD schemes, including the optimum MUD and the joint/separate minimum mean-square error (MMSE) MUDs. Our study shows that the iterative TF-domain MUD is capable of achieving nearly the same BER performance as the optimum MUD, but at much lower complexity.**

I. Introduction

Recently, multicarrier CDMA using both Time (T)-domain and Frequency (F)-domain spreading, namely the TF/MC DS-CDMA, has attracted wide attention in the field of broadband wireless communications [1–5]. More explicitly, in the TF/MC DS-CDMA the transmitted data stream is spread using two signature sequences, one implements the T-domain spreading and the other once implements the F-domain spreading [1, 3]. The benefits of employing both T-domain spreading and F-domain spreading in the TF/MC DS-CDMA systems are multi-fold. Firstly, the TF/MC DS-CDMA uses relatively lower chip-rate and shorter spreading sequences than the conventional single-carrier DS-CDMA [2]. Hence, relatively low-rate signal processing techniques may be used for implementation of the TF/MC DS-CDMA. Secondly, owing to employing both the T-domain and F-domain spreading, the maximum number of users supportable by the TF/MC DS-CDMA does not have to make a trade-off with the frequency-diversity achieved by using F-domain repetition [4]. Furthermore, in the TF/MC DS-CDMA users can be distinguished either by their T-domain signatures or by their F-domain signatures, or by their joint TF-domain signatures. Therefore, signal detection in the TF/MC DS-CDMA has a high-flexibility, which may provide the design of wireless communications systems a good trade-off between complexity and achievable BER performance [2, 3, 5].

In this contribution we propose and investigate an iterative TF-domain MUD scheme for the TF/MC DS-CDMA, when communicating over multipath Rayleigh fading channels. The proposed iterative TF-domain MUD consists of a group of T-domain SISO-MUDs and a group of F-domain SISO-MUDs. Both the T-domain and F-domain SISO-MUDs are operated under the MAP principles. The T-domain SISO-MUDs and F-domain SISO-MUDs are connected through two group-level interference cancellation (GIC) units, where MUI cancellation [6, 7] is attempted. In this contribution the BER performance of the TF/MC DS-CDMA systems using the proposed iterative TF-domain MUD is investigated, when communicating over multipath Rayleigh fading channels. The BER performance and complexity of the proposed iterative TF-domain MUD are compared with the other existing MUD schemes, which include the optimum MUD [8], the joint and separate MMSE-MUDs [3, 4]. Our study and simulation results show that the iterative TF-domain MUD is capable of achieving a similar BER performance as the optimum MUD. However, the detection complexity of the iterative TF-domain MUD is significantly lower than that of the optimum MUD.

II. Time-Frequency-Domain Spread Multicarrier DS-CDMA

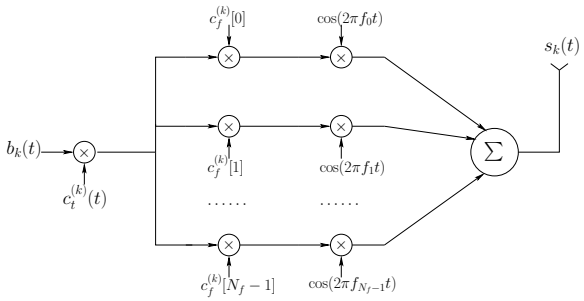

Fig. 1. Transmitter model of MC DS-CDMA using both time- and frequence-domain spreading.

A. Transmitted Signal

The transmitter schematic block diagram for the kth uplink user supported by the TF/MC DS-CDMA is shown in Fig. 1.

For the sake of convenience, the main parameters used in this contribution are summarized as follows:

- N_f: Number of orthogonal subcarriers or F-domain spreading factor;
- T_b, T_c: Bit duration and chip duration;
- N_t: T-domain spreading factor, $N_t = T_b/T_c$;
- N: Number of T-domain spreading sequences assigned to the users supported by the TF/MC DS-CDMA system, $1 < N \leq N_t$;
- M: Number of F-domain spreading sequences assigned to the users supported by the TF/MC DS-CDMA system, $1 < M \leq N_f$;
- K: Number of users supported by the TF/MC DS-CDMA system. It is assumed that $K = MN$. However, if the number of active users dose not meet this assumption, some virtual users, which do not transmit data, are added to make $K = MN$.

For simplicity, in this contribution we assume that the binary phase-shift keying (BPSK) baseband modulation is employed. As shown in Fig. 1, the binary data stream $b_k(t)$ is first DS spread using the T-domain signature sequence $c_t^{(k)}(t)$. Following the T-domain spreading, F-domain spreading using the F-domain spreading sequence $\mathbf{c}_f^{(k)} = \left[c_{f0}^{(k)}, c_{f1}^{(k)}, \cdots, c_{f(N_f-1)}^{(k)}\right]^T / \sqrt{N_f}$, and multicarrier modulation are carried out, yielding the kth user's transmitted signal, which can be expressed as

$$s_k(t) = \Re\left\{\sqrt{\frac{2P}{N_f}} \sum_{i=0}^{N_f-1} b_k(t) c_t^{(k)}(t) c_{fi}^{(k)} \exp[j(\omega_i t + \phi_{ki})]\right\} \quad (1)$$

where P represents the transmission power, $\omega_i = 2\pi f_i$ and f_i is the frequency of the ith subcarrier, while ϕ_{ki} is the associated initial phase. In (1) $b_k(t) = \sum_{j=0}^{\infty} b_{kj} P_{T_b}(t - jT_b)$ denote the binary data waveform consisting of a sequence of mutually independent rectangular pulses of duration T_b and amplitude $+1$ or -1, $c_t^{(k)}(t)$ is the DS spread-spectrum waveform formed from the T-domain sequence $\mathbf{c}_t^{(k)} = \left[c_{t0}^{(k)}, c_{t1}^{(k)}, \cdots, c_{t(N_t-1)}^{(k)}\right]^T / \sqrt{N_t}$.

In this contribution random T-domain and F-domain spreading sequences are assumed, implying that both $c_{tj}^{(k)}$ and $c_{fi}^{(k)}$ take values in $\{+1, -1\}$ with equally probability. Let $\left\{\boldsymbol{c}_t^{(1)}, \boldsymbol{c}_t^{(2)}, \cdots, \boldsymbol{c}_t^{(N)}\right\}$ and $\left\{\mathbf{c}_f^{(1)}, \mathbf{c}_f^{(2)}, \cdots, \mathbf{c}_f^{(M)}\right\}$ be the N number of T-domain spreading sequences and M number of F-domain spreading sequences, respectively, for supporting the $K = MN$ number of active users. Then, the T-domain spreading sequence $\mathbf{c}_t^{(n)}$ is assigned to the kth user, if $n = k - \lfloor k/N \rfloor N$, and the F-domain spreading sequence $\mathbf{c}_f^{(m)}$ is assigned to the kth user, if $m = \lfloor k/N \rfloor + 1$, where $\lfloor x \rfloor$ represents the largest integer less than x. Consequently, Equation (1) can be expressed in terms of m and n as

$$s_{mn}(t) = \Re\left\{\sqrt{\frac{2P}{N_f}} \sum_{i=0}^{N_f-1} b_k(t) c_t^{(n)}(t) c_{fi}^{(m)} \exp[j(\omega_i t + \phi_{ki})]\right\}$$
$$k = mn; m = 1, \ldots, M; n = 1, \ldots, N \quad (2)$$

B. Channel Model

We assume a frequency-selective Rayleigh fading channel, which, corresponding to the kth user, has the T-domain channel impulse response (CIR) of

$$\bar{h}_k(t) = \sum_{l=0}^{L-1} \bar{h}_l^{(k)} \delta(t - \tau_{kl}) \quad (3)$$

where L represents the number of T-domain resolvable multipaths, $\bar{h}_l^{(k)}$ is the channel gain of the lth resolvable multipath, which obey the complex Gaussian distribution with mean zero and a variance $0.5/L$ per dimension.

In MC DS-CDMA it is reasonable to assume that each subcarrier experiences frequency non-selective fading, which can be achieved by correspondingly configuring the number of subcarriers and the bandwidth occupied by each subcarrier [3]. Specifically, the condition for each subcarrier to experience frequency non-selective fading can be guaranteed, provided that the number of T-domain resolvable multipaths satisfies $L \leq N_f/2$. Furthermore, we assume that in our TF/MC DS-CDMA multicarrier modulation/demodulation are implemented using the IFFT/FFT techniques and cyclic-prefixing is employed for removing the inter-block interference. Based on the above assumptions, it can be shown that the F-domain CIRs associated with the N_f subcarriers can be expressed in vector form as [3]

$$\boldsymbol{h}_k = \left[h_0^{(k)}, h_1^{(k)}, \cdots, h_{N_f-1}^{(k)}\right]^T = \sqrt{N_f} \mathcal{F} \bar{\boldsymbol{h}}_k \quad (4)$$

where $\mathcal{F}$ denotes a normalized FFT matrix satisfying $\boldsymbol{\mathcal{F}}\boldsymbol{\mathcal{F}}^H = \boldsymbol{\mathcal{F}}^H\boldsymbol{\mathcal{F}} = \boldsymbol{I}_{N_f}$, while $\bar{\boldsymbol{h}}_k$ is a N_f-length vector formed from the T-domain CIRs shown in (3), $\bar{\boldsymbol{h}}_k = \left[\bar{h}_0^{(k)}, \bar{h}_1^{(k)}, \cdots, \bar{h}_{L-1}^{(k)}, 0, \cdots, 0\right]^T$.

C. Received Signal

We assume that the TF/MC DS-CDMA system supports K number of synchronous users. The power received from each of the K users is assumed to be identical, implying perfect power control. Then, after removing the cyclic prefixing and FFT-based multicarrier demodulation, the $N_f N_t$-length observation vector $\boldsymbol{r}$ obtained from the N_f number of subcarrier channels can be expressed as

$$\begin{aligned}\boldsymbol{r} &= \sum_{k=1}^{K} \left[\left(\boldsymbol{c}_f^{(k)} \odot \boldsymbol{h}_k\right) \otimes \boldsymbol{c}_t^{(k)}\right] b_k + \boldsymbol{n} \\ &= \sum_{m=1}^{M} \sum_{n=1}^{N} \left[\left(\boldsymbol{c}_f^{(m)} \odot \boldsymbol{h}_{mn}\right) \otimes \boldsymbol{c}_t^{(n)}\right] b_{mn} + \boldsymbol{n} \\ &= \sum_{m=1}^{M} \sum_{n=1}^{N} \boldsymbol{H}_{mn} b_{mn} + \boldsymbol{n} \end{aligned} \quad (5)$$

where $\odot$ and $\otimes$ denote the *Hadamard product* and *Kronecker product* operations, respectively and, by definition, $\boldsymbol{H}_{mn} = \left(\boldsymbol{c}_f^{(m)} \odot \boldsymbol{h}_{mn}\right) \otimes \boldsymbol{c}_t^{(n)}$. Furthermore, in (5) $\boldsymbol{n}$ is a $N_t N_f$-length Gaussian noise vector, which obeys the Gaussian distribution with mean zero and a covariance matrix $\sigma^2 \boldsymbol{I}$, where $\sigma^2 = N_0/E_b$ with E_b and N_0 denoting the energy per bit and single-side power spectral density (PSD) of the Gaussian noise process.

It can be readily shown that (5) can be expressed in a compact form as

$$\boldsymbol{r} = \boldsymbol{H}\boldsymbol{b} + \boldsymbol{n} \tag{6}$$

after defining

$$\boldsymbol{b} = [b_{11}, b_{12}, \cdots, b_{1N}; \cdots; b_{M1}, b_{M2}, \cdots, b_{MN}]^T \tag{7}$$

$$\boldsymbol{H} = [\boldsymbol{H}_{11}, \boldsymbol{H}_{12}, \cdots, \boldsymbol{H}_{1N}; \cdots; \boldsymbol{H}_{M1}, \boldsymbol{H}_{M2}, \cdots, \boldsymbol{H}_{MN}] \tag{8}$$

where $\boldsymbol{H}$ is a $(N_f N_t \times MN)$ matrix.

Let assume that the base-station (BS) receiver employs the knowledge about $\boldsymbol{H}$. Then, the sufficient statistics for detection of $\boldsymbol{b}$ can be formed as

$$\boldsymbol{y} = \boldsymbol{H}^H \boldsymbol{r} = \boldsymbol{R}\boldsymbol{b} + \boldsymbol{n}' \tag{9}$$

where

$$\boldsymbol{y} = [y_{11}, y_{12}, \cdots, y_{1N}; \cdots; y_{M1}, y_{M2}, \cdots, y_{MN}]^T \tag{10}$$

is a $K(=MN)$-length vector, $\boldsymbol{R} = \boldsymbol{H}^H\boldsymbol{H}$ is the $(K \times K)$ correlation matrix and $\boldsymbol{n}' = \boldsymbol{H}^H\boldsymbol{n}$, which is Gaussian distributed with mean zero and a covariance matrix $\sigma^2\boldsymbol{R}$.

According to the spreading sequence assignment scheme stated in Section II-A, the $K = MN$ active users share N number of T-domain spreading sequences and M number of F-domain spreading sequences. Hence, the K number of users can either be divided into M groups, where each group contains N number of users sharing one common F-domain spreading sequence but assigned different T-domain spreading sequences, or be divided into N groups, where each group contains M number of users sharing one common T-domain spread sequence but assigned different F-domain spreading sequence. Hence, for convenience of carrying out iterative TF-domain detection, we can use the entries of $\boldsymbol{y}$ to form a $(N \times M)$ matrix $\boldsymbol{Y}$, which is given by

$$\begin{aligned}\boldsymbol{Y} &= \begin{bmatrix} y_{11} & y_{21} & \cdots & y_{M1} \\ y_{12} & y_{22} & \cdots & y_{M2} \\ \vdots & \vdots & \ddots & \vdots \\ y_{1N} & y_{2N} & \cdots & y_{MN} \end{bmatrix} \\ &= [\boldsymbol{y}_{t1}, \boldsymbol{y}_{t2}, \cdots, \boldsymbol{y}_{tM}] \\ &= [\boldsymbol{y}_{f1}, \boldsymbol{y}_{f2}, \cdots, \boldsymbol{y}_{fN}]^T \end{aligned} \tag{11}$$

where different columns correspond to different F-domain spreading sequences, while different rows correspond to different T-domain spreading sequences. Specifically, $\boldsymbol{y}_{tm} = [y_{m1}, y_{m2}, \cdots, y_{mN}]^T$, $m = 1, 2, \ldots, M$, corresponds to a group of N users sharing the mth F-domain spreading sequence, while $\boldsymbol{y}_{fn} = [y_{1n}, y_{2n}, \cdots, y_{Mn}]^T$, $n = 1, 2, \ldots, N$, corresponds to a group of M users sharing the nth T-domain spreading sequence. Let us now derive the iterative TF-domain multiuser detection in the next section.

III. Iterative TF-domain Multiuser Detection

A. Iterative Multiuser Receiver Structure

The receiver structure for iterative TF-domain MUD of TF/MC DS-CDMA signals is shown in Fig. 2. As shown in Fig. 2, the input to the iterative TF-domain MUD is $\boldsymbol{Y}$ given by (11). The iterative TF-domain MUD consists of two main components, the T-domain MUD containing M number of T-domain SISO-MUDs and the F-domain MUD containing N number of F-domain SISO-MUDs. The T-domain MUD and F-domain MUD are separated by two group interference cancellers (GICs), which are the GIC1 and GIC2, respectively, as seen in Fig. 2.

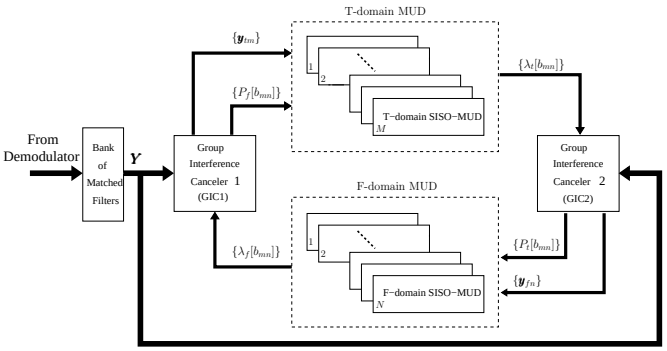

Fig. 2. Receiver model for the TF/MC DS-CDMA using iterative TF-domain multiuser detection.

The inputs to the M number of T-domain SISO-MUDs of Fig. 2 are $\{\boldsymbol{y}_{tm}, m = 1, \cdots, M\}$ seen in (11). Each of the T-domain SISO-MUDs tries to suppress the MUI existing among the users in same group, while treating the MUI from the other groups as noise. Specifically, based on $\boldsymbol{y}_{tm}$ and possible *a-priori* knowledge, the mth T-domain SISO-MUD calculates the *a posteriori* log-likelihood ratios (LLRs) for the bits $\{b_{mn}, n = 1, 2, \ldots, N\}$ transmitted by the N users of the mth group, according to the formula

$$\Lambda_t[b_{mn}] = \log \frac{P[b_{mn} = +1|\boldsymbol{y}_{tm}]}{P[b_{mn} = -1|\boldsymbol{y}_{tm}]},\ n = 1, 2, \ldots, N;\quad m = 1, 2, \ldots, M \tag{12}$$

Similarly, the inputs to the N number of F-domain SISO-MUDs of Fig. 2 are $\{\boldsymbol{y}_{fn}, n = 1, \cdots, N\}$. Based on $\boldsymbol{y}_{fn}$ and possible *a-priori* knowledge, the nth F-domain SISO-MUD calculates the *a posteriori* LLRs for the bits $\{b_{mn}, m = 1, 2, \ldots, M\}$ transmitted by the M users of the nth group, according to the formula

$$\Lambda_f[b_{mn}] = \log \frac{P[b_{mn} = +1|\boldsymbol{y}_{fn}]}{P[b_{mn} = -1|\boldsymbol{y}_{fn}]},\ m = 1, 2, \ldots, M;\quad n = 1, 2, \ldots, N \tag{13}$$

As shown in Fig. 2, the T-domain MUD and F-domain MUD exchange information through two GICs of GIC1 and GIC2, where the K users are regrouped and group-level interference cancellation is carried out.

In more detail, the proposed iterative TF-domain MUD is operated as follows:

1) At the start of the iterative MUD, the sufficient statistics of $\boldsymbol{Y}$ are input to both the GIC1 and GIC2, where $\boldsymbol{Y}$ is divided into M sets of $\{\boldsymbol{y}_{tm}, m = 1, \cdots, M\}$ by GIC1 and divided into N sets of $\{\boldsymbol{y}_{fn}, n = 1, \cdots, N\}$ by GIC2. Then, $\{\boldsymbol{y}_{tm}, m = 1, \cdots, M\}$ are sent to the M number of T-domain SISO-MUDs as seen in Fig. 2.

2) In the first iteration, based on $\{\boldsymbol{y}_{tm}, m = 1, \cdots, M\}$, the M number of T-domain SISO-MUDs as seen in Fig. 2 compute the LLRs $\{\lambda_t[b_{mn}]\}$ using (12) for the $K = MN$ data bits in $\boldsymbol{b}$ by assuming that there is no *a-priori* information. The LLRs are then sent to GIC2, where they are divided into N sets corresponding to $\{\boldsymbol{y}_{fn}, n = 1, \cdots, N\}$. At GIC2, group-level interference cancellation is carried out, which updates $\{\boldsymbol{y}_{fn}, n = 1, \cdots, N\}$ using the soft estimates $\{\lambda_t[b_{mn}]\}$, as will be detailed in our forthcoming discourse. After the group-level interference cancellation, the updated version of $\{\boldsymbol{y}_{fn}, n = 1, \cdots, N\}$ and the *a-priori* $\{P_t[b_{mn}]\}$ are sent to the N number of F-domain SISO-MUDs as shown in Fig. 2. Based on $\{\boldsymbol{y}_{fn}, n = 1, \cdots, N\}$ and $\{P_t[b_{mn}]\}$, finally, the F-domain SISO-MUDs compute the LLRs $\{\lambda_f[b_{mn}]\}$ using (13) for the $K = MN$ data bits of $\boldsymbol{b}$.
3) In the following iterations, both GIC1 and GIC2 employ the *a-priori* information. Hence, both GIC1 and GIC2 can be operated in the similar way as that of GIC2 in step 2): they first carry out the group-level interference cancellation to form the updated versions of $\{\boldsymbol{y}_{tm}, m = 1, \cdots, M\}$ and $\{\boldsymbol{y}_{fn}, n = 1, \cdots, N\}$, which are then sent to the T-domain and F-domain SISO-MUDs, respectively, associated with the corresponding *a-priori* information. At the T-domain and F-domain SISO-MUDs, the LLRs are then updated based on (12) and (13), respectively.
4) Finally, when a sufficient number of iterations are operated yielding a converged BER performance, or the maximum number of iterations is reached, the transmitted data bits can be estimated as the signs of the LLRs obtained either from the M number of T-domain SISO-MUDs or from the N number of F-domain SISO-MUDs.

Below we analyze the principles of the SISO-MUDs and group-level interference cancellation.

B. Soft-Input Soft-Output Multiuser Detection

The T-domain and F-domain SISO-MUDs considered in this contribution are similar as that proposed in [7]. In detail, for the T-domain SISO-MUDs, using the Bayes' rule [3], we can express (12) as

$$\Lambda_t[b_{mn}] = \log \frac{P[\boldsymbol{y}_{tm}|b_{mn} = +1]}{P[\boldsymbol{y}_{tm}|b_{mn} = -1]} + \log \frac{P[b_{mn} = +1]}{P[b_{mn} = -1]} \quad (14)$$

where the second item at the righthand side represents the *a priori* LLR of bit b_{mn}, which is provided by the F-domain SISO-MUDs in the last iteration. By contrast, the first item at the righthand side of (14), which is denoted by $\lambda_t[b_{mn}]$, is the extrinsic information provided by the T-domain SISO-MUDs based on the statistics $\boldsymbol{Y}$.

It can be shown that the statistics $\boldsymbol{y}_{ti}$ in (11) for the ith group of users can be written as

$$\boldsymbol{y}_{ti} = \boldsymbol{R}_{ti}\boldsymbol{b}_i + \sum_{\substack{m=1 \\ m\neq i}}^{M} \boldsymbol{R}_{tm}\boldsymbol{b}_m + \boldsymbol{n}_i,\ i = 1, 2, \ldots, M \quad (15)$$

where

$$\begin{aligned} \boldsymbol{b}_m &= [b_{m1}, b_{m2}, \cdots, b_{mN}]^T \\ \boldsymbol{R}_{tm} &= [\boldsymbol{H}_{i1}, \boldsymbol{H}_{i2}, \cdots, \boldsymbol{H}_{iN}]^H [\boldsymbol{H}_{m1}, \boldsymbol{H}_{m2}, \cdots, \boldsymbol{H}_{mN}] \end{aligned} \quad (16)$$

and $\boldsymbol{n}_i$ is a zero-mean Gaussian random vector distributed with a covariance matrix $\sigma^2\boldsymbol{R}_{ti}$. As mentioned previously in Section III-A, the statistics input to the T-domain SISO-MUDs represent the modified version of $\boldsymbol{y}_{ti}$ upon invoking the group-level interference cancellation. The modified version of $\boldsymbol{y}_{ti}$ for $i = 1, 2, \ldots, M$ is formed as

$$\begin{aligned} \boldsymbol{y}_{ti} &\leftarrow \boldsymbol{y}_{ti} - \sum_{\substack{m=1 \\ m\neq i}}^{M} \boldsymbol{R}_{tm}\hat{\boldsymbol{b}}_m \\ &= \boldsymbol{R}_{ti}\boldsymbol{b}_i + \sum_{\substack{m=1 \\ m\neq i}}^{M} \boldsymbol{R}_{tm}(\boldsymbol{b}_m - \hat{\boldsymbol{b}}_m) + \boldsymbol{n}_i \end{aligned} \quad (17)$$

where $\hat{\boldsymbol{b}}_m$ denotes the soft estimate of $\boldsymbol{b}_m$, which is given in (29) obtained from the last iteration. Note that, when there is no *a-priori* information at the first iteration, we set $\hat{\boldsymbol{b}}_m = \boldsymbol{0}$.

Based on (17), the extrinsic information $\lambda_t[b_{ij}]$ in (14) can now be computed using the formula [7]

$$\lambda_t[b_{ij}] = \log \frac{\sum_{\boldsymbol{b}\in\boldsymbol{b}^+} \exp\left[-(\boldsymbol{y}_{ti} - \boldsymbol{R}_{ti}\boldsymbol{b})^H \boldsymbol{C}_t^{-1}(\boldsymbol{y}_{ti} - \boldsymbol{R}_{ti}\boldsymbol{b})\right] \prod_{n\neq j} P_f[b_{in}]}{\sum_{\boldsymbol{b}\in\boldsymbol{b}^-} \exp\left[-(\boldsymbol{y}_{ti} - \boldsymbol{R}_{ti}\boldsymbol{b})^H \boldsymbol{C}_t^{-1}(\boldsymbol{y}_{ti} - \boldsymbol{R}_{ti}\boldsymbol{b})\right] \prod_{n\neq j} P_f[b_{in}]} \quad (18)$$

where the probabilities $\{P_f[b_{in}]\}$ are given in (29) and, by definition,

$$\begin{aligned} \boldsymbol{b}^+ &= [b_{i1}, \cdots, b_{i(j-1)}, +1, b_{i(j+1)}, \cdots, b_{iN}] \\ \boldsymbol{b}^- &= [b_{i1}, \cdots, b_{i(j-1)}, -1, b_{i(j+1)}, \cdots, b_{iN}] \end{aligned} \quad (19)$$

The covariance matrix $\boldsymbol{C}_t$ in (18) can be evaluated with the aid of (17). Remembering that the MUI caused by other user groups is treated as Gaussian noise and that the transmitted bits are assumed to be independent, $\boldsymbol{C}_t$ can hence be expressed as

$$\boldsymbol{C}_t = \sum_{\substack{m=1 \\ m\neq i}}^{M} \left(\boldsymbol{R}_{tm}\text{cov}\{\boldsymbol{b}_m - \hat{\boldsymbol{b}}_m\}\boldsymbol{R}_{tm}^H\right) + \sigma^2\boldsymbol{R}_{ti} \quad (20)$$

where $\text{cov}\{\boldsymbol{b}_m - \hat{\boldsymbol{b}}_m\}$ is the covariance matrix of $(\boldsymbol{b}_m - \hat{\boldsymbol{b}}_m)$, which can be expressed as

$$\text{cov}\{\boldsymbol{b}_m - \hat{\boldsymbol{b}}_m\} = \text{diag}\left\{1 - \hat{b}_{m1}^2, 1 - \hat{b}_{m2}^2, \cdots, 1 - \hat{b}_{mN}^2\right\} \quad (21)$$

As shown in Fig. 2, the extrinsic information $\{\lambda_t[b_{ij}]\}$ is sent to the GIC2. Based on (18), GIC2 evaluates the probability of the event that $b_{mn} = +1$ or -1, which can be expressed as [7]

$$\begin{aligned} P_t[b_{mn}] = \frac{1}{2}\left[1 + b_{mn}\tanh\left(\frac{1}{2}\lambda_t[b_{mn}]\right)\right], \\ m = 1, \ldots, M;\ n = 1, \ldots, N \end{aligned} \quad (22)$$

Note that, the probabilities $\{P_t[b_{mn}]\}$ represent the *a-priori* probabilities for the following F-domain MUD. GIC2 also evaluates the soft estimate to b_{mn}, which can be denoted as [7]

$$\hat{b}_{mn} = \tanh\left(\frac{1}{2}\lambda_t[b_{mn}]\right),\ m = 1,\ldots,M;\ n = 1,\ldots,N \tag{23}$$

The estimates of $\{\hat{b}_{mn}\}$ are used by GIC2 for implementation of the group-level interference cancellation, which, for $j = 1, 2, \ldots, N$, can be formulated as

$$\boldsymbol{y}_{fj} \leftarrow \boldsymbol{R}_{fj}\boldsymbol{b}_j + \sum_{\substack{n=1 \\ n\neq j}}^{N} \boldsymbol{R}_{fn}(\boldsymbol{b}_n - \hat{\boldsymbol{b}}_n) + \boldsymbol{n}_j \tag{24}$$

where $\boldsymbol{b}_n = [b_{1n}, b_{2n}, \cdots, b_{Mn}]^T$ and $\hat{\boldsymbol{b}}_n$ denotes its soft estimation according to (23). Furthermore, in (24)

$$\boldsymbol{R}_{fn} = [\boldsymbol{H}_{1j}, \boldsymbol{H}_{2j}, \cdots, \boldsymbol{H}_{Mj}]^H [\boldsymbol{H}_{1n}, \boldsymbol{H}_{2n}, \cdots, \boldsymbol{H}_{Mn}] \tag{25}$$

and $\boldsymbol{n}_j$ is a zero-mean Gaussian random vector associated with a covariance matrix of $\sigma^2\boldsymbol{R}_{fj}$.

Let us now turn to consider the F-domain SISO-MUDs, which are operated in similar approaches as the above-analyzed T-domain SISO-MUDs. As shown in Fig. 2, the F-domain SISO-MUDs accept the inputs of $\{\boldsymbol{y}_{fj}\}$ and $\{P_t[b_{ij}]\}$ and compute the extrinsic information $\{\lambda_f[b_{ij}]\}$ according to the formula

$$\lambda_f[b_{ij}] = \log \frac{\sum_{\boldsymbol{b}\in\boldsymbol{b}^+} \exp[-(\boldsymbol{y}_{fj} - \boldsymbol{R}_{fj}\boldsymbol{b})^H \boldsymbol{C}_f^{-1}(\boldsymbol{y}_{fj} - \boldsymbol{R}_{fj}\boldsymbol{b})] \prod_{m\neq i} P_t[b_{mj}]}{\sum_{\boldsymbol{b}\in\boldsymbol{b}^-} \exp[-(\boldsymbol{y}_{fj} - \boldsymbol{R}_{fj}\boldsymbol{b})^H \boldsymbol{C}_f^{-1}(\boldsymbol{y}_{fj} - \boldsymbol{R}_{fj}\boldsymbol{b})] \prod_{m\neq i} P_t[b_{mj}]} \tag{26}$$

where, upon following (18), we have

$$\begin{aligned} \boldsymbol{b}^+ &= [b_{1j}, \cdots, b_{(i-1)j}, +1, b_{(i+1)(j)}, \cdots, b_{Mj}] \\ \boldsymbol{b}^- &= [b_{1j}, \cdots, b_{(i-1)j}, -1, b_{(i+1)(j)}, \cdots, b_{Mj}] \end{aligned} \tag{27}$$

$$\boldsymbol{C}_f = \sum_{\substack{n=1 \\ n\neq j}}^{N} \left(\boldsymbol{R}_{fn}\mathrm{cov}\{\boldsymbol{b}_n - \hat{\boldsymbol{b}}_n\}\boldsymbol{R}_{fn}^H\right) + \sigma^2\boldsymbol{R}_{fj} \tag{28}$$

Furthermore, upon receiving $\{\lambda_f[b_{ij}]\}$, GIC1 can evaluate $\{P_f[b_{mn}]\}$ and $\{\hat{b}_{mn}\}$ as

$$\begin{aligned} P_f[b_{mn}] &= \frac{1}{2}\left[1 + b_{mn}\tanh\left(\frac{1}{2}\lambda_f[b_{mn}]\right)\right] \\ \hat{b}_{mn} &= \tanh\left(\frac{1}{2}\lambda_f[b_{mn}]\right) \end{aligned} \tag{29}$$

for $m = 1,\ldots,M;\ n = 1,\ldots,N$. These quantities are then sent to the T-domain MUDs for carrying out the next iteration of MUD, as shown in (18).

C. Detection Complexity

It is well-known that the optimum MUDs have a complexity on the order of $\mathcal{O}\left(2^K\right)$ [8]. Therefore, the complexity of the optimum MUDs might be extreme if the number of users K is relatively high, which consequently limits the application of the optimum MUDs. In the proposed iterative TF-domain MUD, the total $K = MN$ number of users supported are either divided into M groups with each group having N users or divided into N groups with each group containing M users. Hence, when optimum MUD is carried out in the context of each of the groups, the complexity is on the order of $\mathcal{O}\left(2^N\right)$ or $\mathcal{O}\left(2^M\right)$. Additionally, it can be shown that in our iterative TF-domain MUD the complexity of GIC1 and GIC2 is on the order of $\mathcal{O}\left(NM^2\right)$ and $\mathcal{O}\left(MN^2\right)$, respectively, in each iteration. Therefore, when considering U iterations, the total complexity for the iterative TF-domain MUD is on the order of $\mathcal{O}\left[U\left(N2^M + M2^N + MN^2 + NM^2\right)\right]$. Hence, when the number of users supported is high, the complexity of the iterative TF-domain MUD may be significantly lower than that of the conventional optimum MUDs. For example, assuming that $K = MN = 8\times 8$ users are supported, the complexity of the conventional optimum MUDs is then on the order of $\mathcal{O}\left(2^{64}\right)$. By contrast, the complexity of the iterative TF-domain MUD is only on the order of $\mathcal{O}\left(2^{14}\right)$, when $U = 4$ iterations are allowed. Note that our simulation results in the next section show that, after $U = 4$ iterations, the iterative TF-domain MUD is generally capable of achieving nearly the same BER performance as the optimum maximum likelihood (ML)-MUD.

IV. Simulation Results

In this section we provide some simulation results in order to illustrate the achievable BER performance of the TF/MC DS-CDMA system using the proposed iterative TF-domain MUD. In our simulations we assumed that the TF/MC DS-CDMA systems had a F-domain spreading factor $N_f = 8$ and a T-domain spreading factor $N_t = 4$. The spreading sequences were random sequences. However, in our simulations different users were assumed not to choose the same T-domain and F-domain spreading sequences. In other words, the user sequences are distinct, when the joint TF-domain is considered.

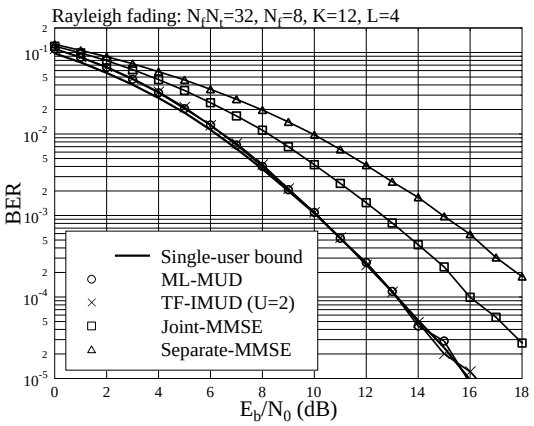

Fig. 3. BER performance comparison of the TF/MC DS-CDMA using various detection schemes, when communicating over Rayleigh fading channels having $L = 4$ T-domain resolvable multipaths.

Fig. 3 compares the BER versus SNR per bit of E_b/N_0 performance of TF/MC DS-CDMA using various detection schemes, when $K = MN = 3\times 4 = 12$ users are supported.

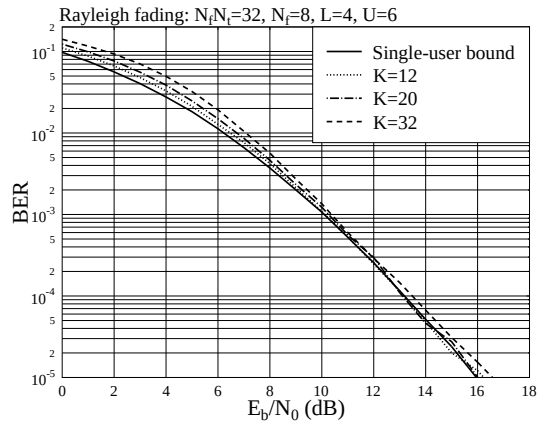

Fig. 4. BER performance comparison of TF/MC DS-CDMA using iterative TF-domain MUD, when communicating over Rayleigh fading channels having $L = 4$ T-domain resolvable multipaths.

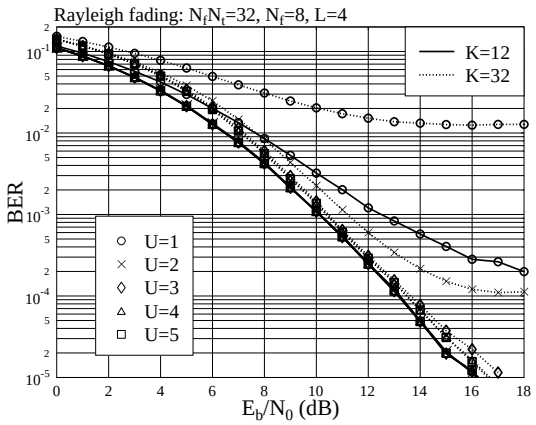

Fig. 5. BER performance comparison of TF/MC DS-CDMA using iterative TF-domain MUD with different number of iterations, when communicating over Rayleigh fading channels having $L = 4$ T-domain resolvable multipaths.

In this figure the joint/separate MMSE-MUDs for the TF/MC DS-CDMA can be found in [3]. Note furthermore that, in the context of the separate MMSE-MUD, the MMSE-MUD is first carried out in the T-domain and followed in the F-domain. From Fig. 3 we observe that both the optimum MUD and iterative TF-domain MUD using two iterations achieve nearly the same BER performance, which is very close to the single-user BER bound. However, as analyzed previously, the complexity of the iterative TF-domain MUD is much lower than that of the optimum MUD. Specifically, the complexity of the optimum MUD is $\mathcal{O}\left(2^{12}\right)$, while the iterative TF-domain MUD is $\mathcal{O}\left(2^{8}\right)$. As shown in Fig. 3, the joint MMSE-MUD outperforms the separate MMSE-MUD, but both of them are outperformed by the optimum MUD or the iterative TF-domain MUD. Note that, the complexity of the joint MMSE-MUD is $\mathcal{O}\left(K^3\right) = \mathcal{O}\left(12^3\right)$, while that of the separate MMSE-MUD is $\mathcal{O}\left(MN^3 + NM^3\right) = \mathcal{O}\left(3 \cdot 4^3 + 4 \cdot 3^3\right)$. Hence, the complexity of the separate MMSE-MUD can be significantly lower than that of the joint MMSE-MUD.

Fig. 4 compares the BER performance of the TF/MC DS-CDMA using iterative TF-domain MUD associated with six iterations, when different number of users are supported. As the results of Fig. 4 shown, even when the TF/MC DS-CDMA system is full-load implying that $K = N_{ft} = 32$, the BER of the TF/MC DS-CDMA is still close to that of the single-user BER bound, especially, when the SNR of E_b/N_0 is relatively high. When the SNR of E_b/N_0 is lower than 9 dB, we can see that BER performance becomes slightly worse, when the number of users supported increases.

Fig. 5 investigates the number of iterations required for achieving the converged BER performance in the TF/MC DS-CDMA systems supporting either $K = 12$ users or $K = 32$ users. From the results of Fig. 5, we can observe that, when $K = 12$ users are supported, the BER performance has nearly no further improvement after two iterations of TF-domain MUD. By contrast, when the system is full-load supporting $K = 32$ users, the BER performance improves as the number of iterations increases before reaching the fourth iteration. As the results of Fig. 5 shown, the BER performance improvement becomes less and less as the number of iterations increases. The reason for the above-mentioned observations is that, when the TF/MC DS-CDMA system is lightly loaded, there is low MUI, which may be sufficiently suppressed after two or three iterations. However, when the TF/MC DS-CDMA system is fully loaded, there is severe MUI. Hence, more iterations of TF-domain MUD are required in order to efficiently remove the MUI. Furthermore, as shown in Fig. 5, when the number of iterations is not sufficient, error-floors are observed owing to the remaining MUI.

In conclusions, our study and simulation results show that the iterative TF-domain MUD is capable of achieving a similar BER performance as the optimum MUD, but with a detection complexity that may be significantly lower than that of the optimum MUD. Owing to its low-complexity and good BER performance, the TF/MC DS-CDMA constitutes one of the promising wireless communications schemes for practical applications.

REFERENCES

[1] C. W. You and D. S. Hong, "Multicarrier CDMA systems using time-domain and frequency-domain spreading codes," *IEEE Transactions on Communications*, vol. 51, no. 1, pp. 17 – 21, January 2003.

[2] L. L. Yang and L. Hanzo, "Multicarrier DS-CDMA: A multiple-access scheme for ubiquitous broadband wireless communications," *IEEE Communications Magazine*, vol. 41, no. 10, pp. 116–124, October 2003.

[3] L.-L. Yang, *Multicarrier Communications*. Chichester, United Kingdom: John Wiley, 2009.

[4] L.-L. Yang, H. Wei, and L. Hanzo, "Multiuser detection assisted time- and frequency-domain spread multicarrier code-division multiple-access," *IEEE Trans. on Veh. Tech.*, vol. 55, no. 1, pp. 397–405, Jan. 2006.

[5] C. W. C. L. C. Wang and H. Huang, "An interference avoidance code assignment strategy for downlink multi-rate MC-DS-CDMA with TF-domain spreading,," *IEEE Transactions on Wireless Communications*, vol. 6, no. 7, pp. 2508 – 2518, July 2007.

[6] U. Madhow and M. L. Honig, "MMSE interference suppression for direct-sequence spread-spectrum CDMA," *IEEE Transactions on Communications*, vol. 42, no. 12, pp. 3178–3188, December 1994.

[7] X. Wang and H. V. Poor, "Iterative (turbo) soft interference cancellation and decoding for coded CDMA," *IEEE Transactions on Communications*, vol. 47, no. 7, pp. 1046 – 1061, July 1999.

[8] S. Verdu, *Multiuser Detection*. Cambridge University Press, 1998.